

Cross-sectional imaging of sinus of Valsalva aneurysms: lessons learned

Mina F. Hanna
Nagina Malguria
Sachin S. Saboo
Kirk G. Jordan
Michael Landay
Brian B. Ghoshhajra
Suhny Abbara

ABSTRACT

Sinus of Valsalva aneurysm, dilatation of one or more of the aortic sinuses, is a rare but important aortic root defect, which can be a cause of some serious cardiac sequels. The purpose of this article is to review the etiopathogenesis, relevant anatomy, clinical manifestations, potential complications, multimodality imaging features, and management of this rare but important entity of sinus of Valsalva.

Sinus of Valsalva (SOV) aneurysm is defined as either the dilatation of one or more of the aortic sinuses located between the aortic valve annulus and the sinotubular junction or a crescentic/tubular-shaped outpouching extending from the body or apex of a normally sized SOV (1–3).

Given the various appearances and difficult location, detection of ruptured and unruptured SOV aneurysms can be a diagnostic challenge. Although, the ruptured SOV aneurysm can be potentially fatal, their prognosis after treatment is excellent. This emphasizes the need for timely accurate diagnosis. In this article, we review the relevant etiopathogenesis, anatomy, clinical manifestations, potential complications, cross-sectional imaging features, and management of this rare but important aortic root defect.

SOV aneurysms prevalence and etiology

Although the precise prevalence of SOV aneurysm is not available, the general population estimate of prevalence is 0.09% (1–5). For etiology, SOV aneurysms are commonly congenital and represent 0.1% to 3.5% of congenital heart defects (6, 7). SOV aneurysm usually originates from the right coronary sinus (70%–90%), followed by the noncoronary sinus (10%–25%) (Fig. 1) and left sinus (<5%) (6). The underlying mechanism for congenital type is incomplete fusion of the distal bulbar septum (primitive bulbis cordis) and truncal ridges (aortopulmonary septum) resulting in fragility at the junction of aortic annulus and the right aortic sinus medias and right portion of the noncoronary sinus (Fig. 2). With continuous pressure over time, this morphologic imperfection leads to an increasing bulge, which can eventually rupture (6, 8).

On the other hand, SOV aneurysms in patients with connective tissue diseases like Marfan syndrome and Loeys-Dietz syndrome cause annuloaortic ectasia resulting in dilatation of all three SOVs and thereby progressive effacement of the sinotubular junction (3). Acquired causes for SOV aneurysms include atherosclerosis, bacterial endocarditis, syphilis, and tuberculosis (3); autoimmune disease such as Behcet's disease (9); degenerative conditions such as cystic medial necrosis; traumatic injury and postoperative after surgical repair of a ventricular septal defect (VSD), aortic valvular diseases, and aortic dissection (3, 6) (Figs. 3, 4).

Normal anatomy and physiology of the aortic root and SOV

The aortic root represents the portion of the aorta and left ventricular outflow tract demarcated by the sinotubular junction superiorly and the basal portions of the aortic valve leaflets inferiorly (Fig. 5). Thus aortic root is made of the aortic valve leaflets, the commis-

From the Department of Radiology, Cardiothoracic Imaging (M.F.H., N.M., S.S.S., K.G.J., M.L., S.A.)
✉ suhny.abbara@utsouthwestern.edu, UT Southwestern Medical Center, Dallas, TX, USA;
Department of Radiology, Cardiothoracic Imaging (M.F.H.), UT Health Science Center, Houston, TX, USA;
Department of Radiology, Cardiac Imaging (B.B.G.) Massachusetts General Hospital, Boston, MA, USA.

Received 23 November 2016; revision requested 14 December 2016; last revision received 23 March 2017; accepted 19 April 2017.

Published online 17 August 2017.
DOI 10.5152/dir.2017.16522

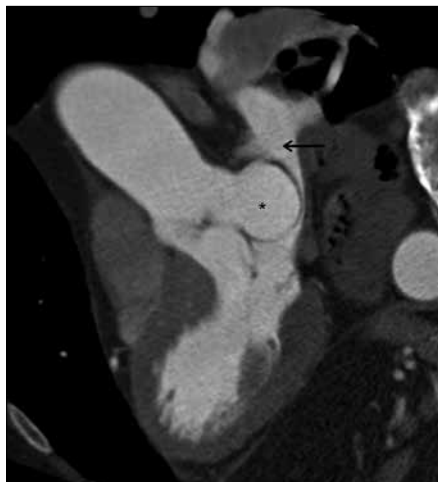


Figure 1. Three-chamber reconstructed view of the heart from electrocardiography (ECG)-gated cardiac CT angiography data demonstrates unruptured aneurysm from the noncoronary sinus of Valsalva (SOV) (black asterisk) protruding into the left atrium (black arrow).

sures, the interleaflet triangles, SOVs, sinotubular junction, and the annulus (10, 11).

SOVs represent the expanded portions. The three sinuses of the aortic root between the attachments of the aortic valve leaflets inferiorly and the sinotubular junction superiorly. Each sinus denotes an aortic valve cusp and the three sinus nomenclature into right, left, and noncoronary sinus is based on the originating coronary artery from it. The noncoronary sinus is located above the interventricular septum and a portion of the anterior mitral leaflet; the right sinus lies in vicinity to the interventricular septum and the right ventricular parietal bands while the left sinus is proximal to the anteri-

or left ventricular free wall and the anterior mitral leaflet (12).

The sinotubular junction, the relatively constricted segment between the aortic root and ascending aorta, is circular and supports the peripheral attachments of the aortic valve leaflets (10).

The aortic valve leaflets hemodynamically separate the aorta from the left ventricle. The nadirs of attachment of the aortic valve leaflets into the wall of the root in a semilunar fashion gives rise to virtual three-dimensional (3D) ring called as aortic annulus (10, 11).

For accurate measurement, normally the SOVs are measured in double short-axis at the aortic root from coronary sinus to its opposite trigon. Another method for measurement of aortic root is named sinus-to-sinus measurement and usually performed from the right coronary sinus to the noncoronary sinus (Fig. 5) (13). A study of 103 patients with electrocardiography (ECG)-gated multidetector computed tomography (CT) has shown normal SOV end diastole measurement as 3.2 ± 0.6 cm for men and 2.9 ± 0.5 cm for women (14). The study showed that aortic root diameter was associated strongly with body size and less strongly with systolic and diastolic blood pressure and stroke volume in univariate analyses, while the root diameter were shown to vary with age and body surface area in multivariate analysis (11).

Functionally, SOVs play an important role in aortic valve function. They provide a space to prevent blocking of the coronary artery orifices from the open aortic leaflets. Secondly, they favor the development of eddy currents behind the open leaflets which in turn hold the leaflets away from the aortic wall in a position where they will be promptly caught and closed by blood flow during end systole (10).

Clinical manifestations and complications of SOV aneurysms

SOV aneurysms may manifest at any age given their congenital and acquired etiologies. The clinical manifestations vary with asymptomatic presentation of the incidentally discovered unruptured aneurysms to severe aortic insufficiency and heart failure of the ruptured aneurysms (15).

Unruptured SOV aneurysms

Overall, unruptured aneurysms are asymptomatic and are incidentally detected during imaging workup of heart murmurs or abnormal cardiomeastinal silhouette on radiograph (16). Rarely, they may present with dyspnea, palpitations, arrhythmias, or angina chest pain. Thrombus can form in large SOV aneurysms (Fig. 6) with subsequent risk

Main points

- Sinus of Valsalva (SOV) aneurysm is dilatation of one or more of the aortic sinuses, which is a rare but important aortic root defect that can be a cause of some serious cardiac sequels.
- SOV aneurysms may manifest at any age given their congenital and acquired etiologies.
- Cross-sectional imaging plays a pivotal role in diagnosis, presurgical planning, and postsurgical follow-up of SOV aneurysms.
- Surgery has been a conventionally and commonly used treatment option for repair of SOV aneurysms; either ruptured or unruptured. However, recently, various percutaneous closure techniques are gaining popularity in certain scenarios.

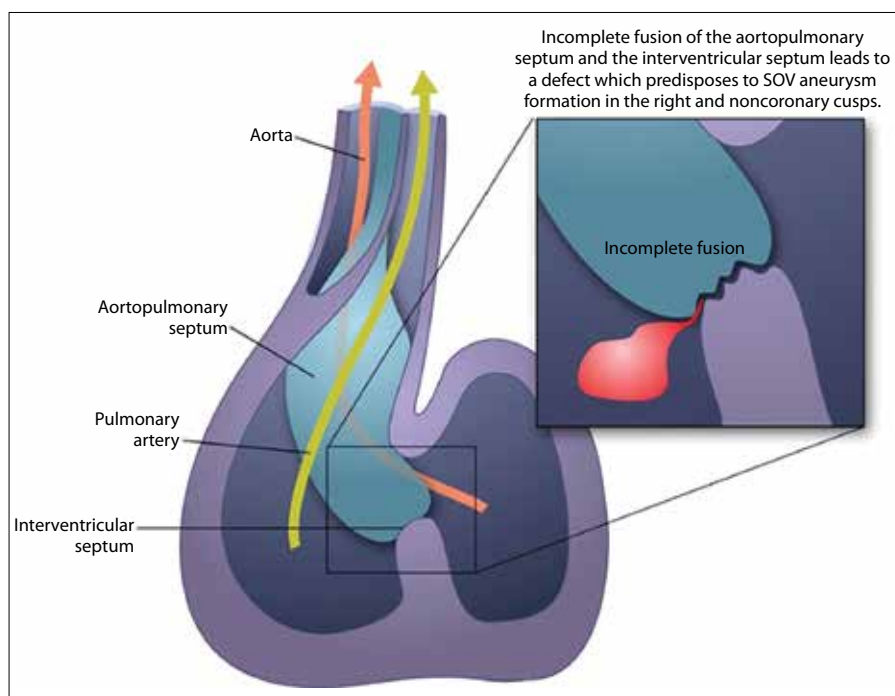


Figure 2. Illustration of the heart and root of aorta showing the pathogenesis for congenital SOV aneurysm.

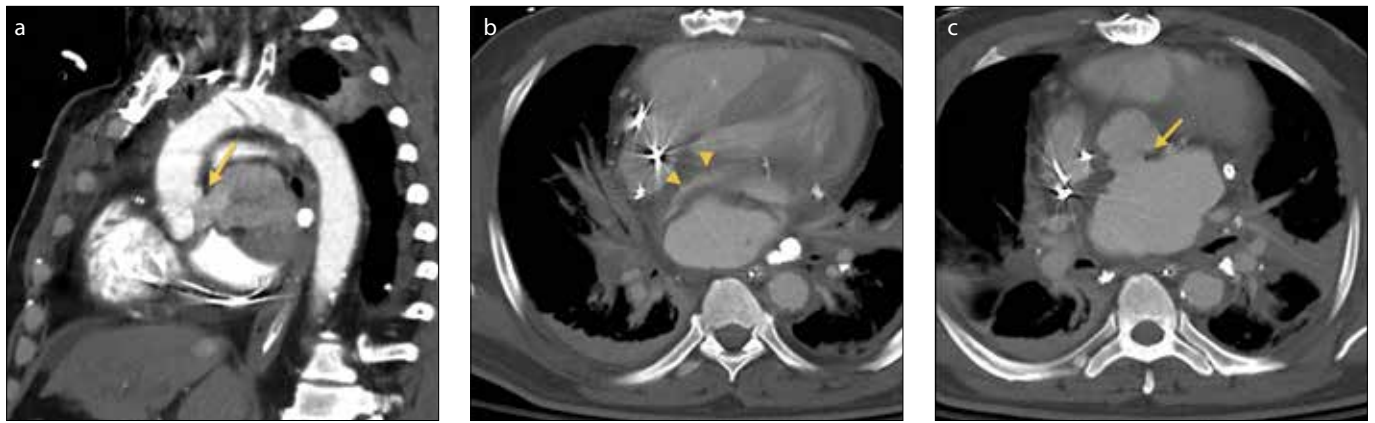


Figure 3. a–c. Acquired post-traumatic SOV pseudoaneurysm in a 56-year-old man. Candy cane multiplanar reconstruction early arterial phase (a) and axial late arterial phase (b, c) contrast-enhanced CT chest images show contained rupture of noncoronary SOV with pseudoaneurysm formation into the oblique pericardial sinus (yellow arrow at the site of rupture) with flattening of the left atrium (yellow arrowheads) due to external compression.

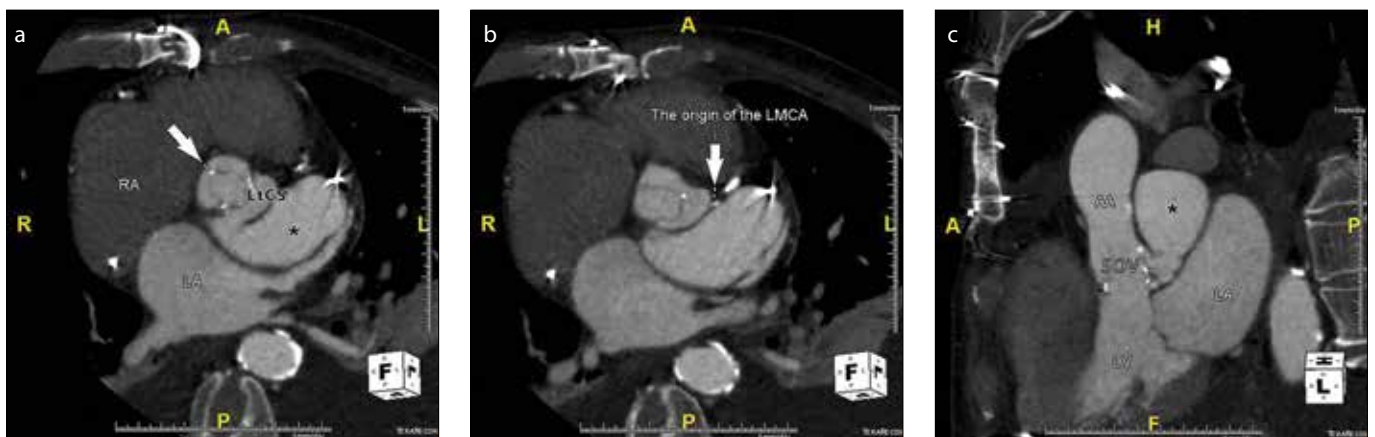


Figure 4. a–c. Acquired SOV pseudoaneurysm (white arrow) in a 67-year-old man following aortic valve replacement. Axial (a, b) and oblique sagittal reconstructed (c) images from contrast-enhanced ECG-gated chest CT show contained rupture of left coronary sinus of Valsalva (Lt CS) with pseudoaneurysm formation (c, white asterisk) into the aortomitral space (black asterisk) with mass effect on the left atrium (LA) posteriorly and left main coronary artery (LMCA) anteriorly due to external compression (AA, ascending aorta; LV, left ventricle; RA, right atrium).

of systemic embolism and stroke (17). Mass effect from large SOV aneurysm can distort or obstruct the coronary ostia thereby leading to myocardial ischemia and infarction (18–20). Both ruptured and unruptured SOV aneurysms can be commonly complicated with aortic regurgitation (AR) which occurs in 30%–50% of patients; therefore requiring aortic valve function evaluation with echocardiogram or magnetic resonance imaging (MRI) (21) and need for aortic valve replacement at the time of surgical fixation of the aneurysm. Based on the location and extent of SOV aneurysm, mass effect on adjacent cardiac structures can occur with impairment in tricuspid and mitral valves function, or partial obstruction of the right ventricular outflow tract. Few case reports describe their rare complications including aneurysmal dissection into the muscular interventricular

septum with resultant arrhythmias, heart block, (22) and infective endocarditis (23).

SOV pseudoaneurysm is extremely rare. It is an outpouching of any of the three SOVs resulting from a deficiency in the tunica media and intima. The vascular lumen is contained by either adventitia only, clotted blood, or surrounding structures. SOV pseudoaneurysm may be spontaneous, traumatic, or infective (24, 25). It can lead to the same complications as the true aneurysm.

Ruptured SOV aneurysms

A ruptured SOV aneurysm is a potentially fatal complication. The size, location, and rapidity of rupture are the major elements predicting clinical consequences. The most common sinus to rupture is right coronary or noncoronary sinuses with the right ventricle being the most common site of rupture (Fig. 7), followed by the right atrium (26, 27).

Other less common sites of rupture in descending order include right ventricular outflow tract, left ventricle, the interventricular septum, left atrium, and extracardiac space (26). Rupture into the extracardiac space although rare has generally higher mortality with critical complications of cardiac tamponade (14). Symptoms of rupture include substernal chest pain, abdominal pain, and dyspnea. Not uncommonly, patients may present with acute heart failure, hemodynamic compromise, or sudden cardiac death (20). Ruptured SOV aneurysms can predispose to formation of para-aortic abscess and endocarditis (15).

Multimodality imaging of SOV aneurysms

SOV aneurysms vary in size from subtle dilatation of an aortic sinus to overt crescentic or windssock-shaped exophytic projection

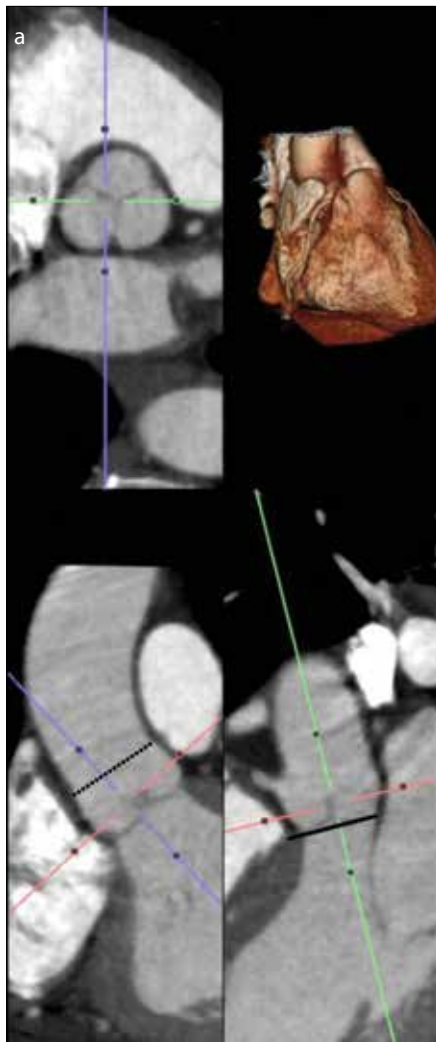


Figure 5. a, b. Normal anatomy of the aortic root in a 48-year-old woman presenting with chest pain. Bottom images (a) demonstrate orthogonal views from an ECG-gated cardiac CT; top left image shows short axis image at the level of the SOVs (dotted black line, sinotubular junction; pink crosshair, sinuses of Valsalva; solid black line, annulus plane). Panel (b) shows orthogonal measurements of the normal SOVs along the short axis plane using sinus-to-trigon (blue line) and sinus-to-sinus (red line) methods.

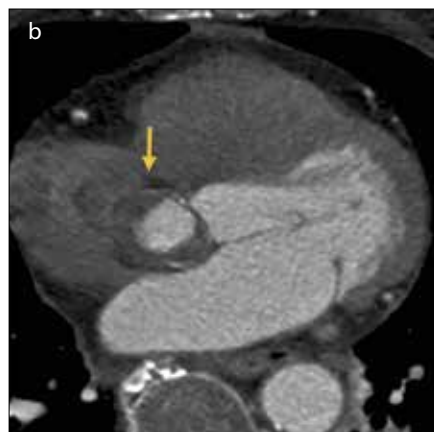
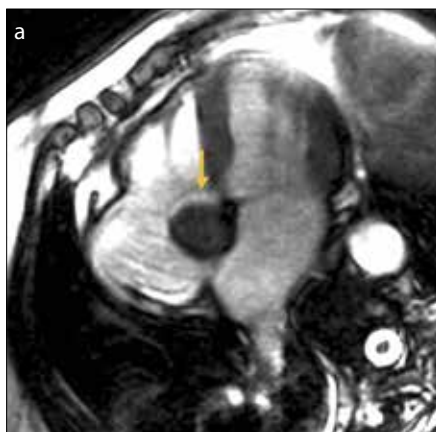


Figure 6. a, b. Thrombosed SOV aneurysm in a 60-year-old woman. Four chamber balanced steady-state free precession (b-SSFP) magnetic resonance image (a) shows predominantly low intensity structure projecting in the interatrial septum (yellow arrow). ECG-gated axial cardiac CT angiography image (b) confirms the MRI finding of SOV aneurysm arising from noncoronary sinus with partial thrombosis and wall calcification (yellow arrow).



Figure 7. A 25-year-old woman with chest pain. Volume rendered oblique sagittal images from an ECG-gated cardiac CT angiography demonstrate ruptured right SOV aneurysm extending from the right coronary sinus into the right ventricle (black arrow).

from the body or apex of the sinus (3). They can also manifest as saccular outpouching or as mass. Many classification methods have been described for SOV aneurysms, with Sakakibara classification of ruptured aneurysms based on originating cusp and the receiving/drainage chamber being the most commonly used method in the surgical literature (Figs. 8-10; Table) (28).

Chest radiograph findings are nonspecific and are based on SOV aneurysm location, size, and presence or absence of rupture. Patients can present with abnormal cardiomeastinal silhouette and minimal to moderate increased pulmonary vascularity. However, patients' right ventricular outflow tract obstruction can manifest with decreased pulmonary vascularity (29).

Conventional angiography, the gold standard test in the past, continues to be used during percutaneous intervention settings (30). However, noninvasive cross-sectional imaging modalities, consisting of echocardiography, cardiac CT, and cardiac MRI have essentially replaced it.

Transthoracic echocardiography is the first screening modality of choice given its good sensitivity, wider availability, and portability (31). Many studies have reported >90% accuracy of echocardiography for detecting the SOV aneurysm with common fallacy being the incorrect detection of the rupture site (23). Transesophageal echocardiography

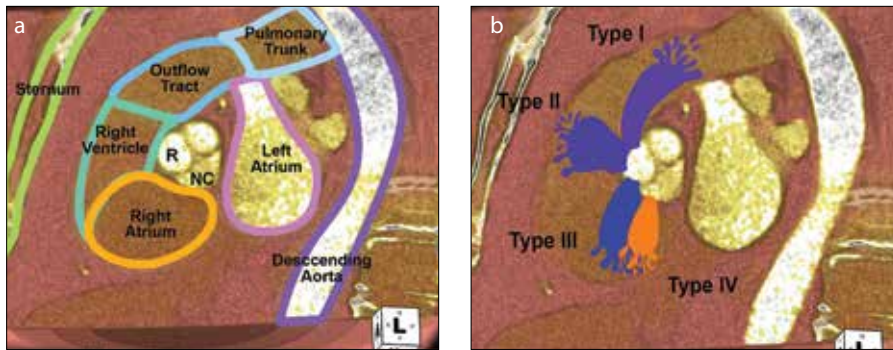


Figure 8. a, b. Illustration of the heart demonstrates Sakakibara classification of ruptured SOV aneurysm. Illustration (a) demonstrates potential different cardiac chambers sites of rupture of SOV aneurysm. R, right coronary sinus; NC, noncoronary sinus. Illustration (b) demonstrates the origin, and the direction of rupture of SOV aneurysm besides the cardiac chamber site of rupture for each SOV aneurysm.

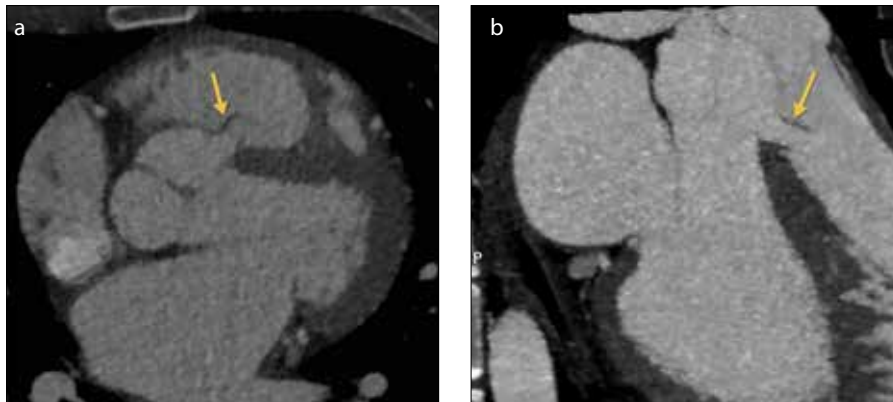


Figure 9. a, b. Sakakibara type II SOV aneurysm originating from the right SOV and rupturing into right ventricle. Axial (a) and 3-chamber reconstructed (b) images of the heart from the ECG-gated cardiac CT angiography data showing the site of rupture of SOV aneurysm (yellow arrow).



Figure 10. Sakakibara type III SOV aneurysm originating from the right SOV and rupturing into right atrium. Coronal oblique reconstructed image from ECG-gated cardiac CT angiography shows the opening/drainage site of the SOV aneurysm (curved white arrow) into the right atrium (RA).

due to its better acoustic window and higher resolution helps in more accurate characterization of the aneurysm (23, 32).

SOV aneurysms may be discovered incidentally on chest CTs performed for other reasons. Contrast-enhanced ECG-gated multidetector cardiac CT angiogram due to its inherent high spatial resolution, improved temporal resolution, wider availability, and rapid scan acquisition is very well suited and commonly used noninvasive modality for evaluation of SOV aneurysms (Fig. 11), cardiac chambers (4, 33) and its relations with the coronary arteries (26, 34).

At our institute, cardiac CT angiography parameters for evaluation of SOV are as follows: given the patient's normal renal functions (eGFR, ≥ 60 mL/min/1.73 m²), 70–100 mL iodinated contrast was given based on the body mass index (BMI) usually through the right antecubital vein with an injection rate of 5–7 mL/s and using triphasic injection technique with dual syringe power injector. The scan length is about 16 cm (carina to apex of heart) and the field-of-view is 25 cm using 80–140 Kvp (depends on the BMI) and 200–500 mAs.

The effective radiation dose depends on the ECG gating technique: it is 1–6 mSv for prospective triggering (during diastole), which is used if there is regular heart rate <65 bpm; but it is 10–15 mSv for retrospective gating, which is used if there is irregular heart rate, heart rate >65 bpm, or if dynamic information about aneurysm filling and emptying or movement in different phases of the cardiac cycle is required.

If retrospective gating is used, tube current dose modulation is performed since dose modulation is known to reduce the radiation dose.

A 64-detector CT scanner or higher detector scanner is the preferred technique and subsequently images are sent to dedicated 3D workstation for multiplanar and volume rendered technique postprocessing for accurate localization, measurement, and for providing road map to clinicians to decide about the management.

Multiphase cardiac MRI plays an important role in the SOV aneurysm assessment due to its lack of ionizing radiation, ability to quantify ventricular functions and aortic regurgitant fraction, better temporal resolution, and assessment of wall motion abnormalities. However, MRI has lower spatial resolution as compared with CT. Combination of various MRI sequences such as balanced steady state free precession (SSFP)/bright blood imaging, single-shot turbo spin-echo, black blood imaging (Fig. 12) and contrast-enhanced magnetic resonance angiography allows accurate assessment of the origin and size of SOV aneurysms, thrombosis of aneurysm, and its relation with the surrounding cardiac and mediastinal structures (4, 30).

SOV aneurysms may be associated with several other congenital cardiac abnormalities (4) and cross-sectional imaging can be useful for their assessment. SOV aneurysms have been associated with bicuspid aortic valves (Fig. 13) in approximately 10% of cases (35). Bicuspid aortic valves due to accelerated degeneration predispose to aortic aortopathy manifesting as aortic valvular stenosis (36), ascending aorta and aortic root dilatation out of proportion to hemodynamic factors, and true SOV aneurysms (37–39). The most commonly reported associations are VSDs (30%–60% of patients). Other associated conditions include aortic insufficiency (20%–30%) (35), aortic stenosis, infundibular pulmonary stenosis, left ventricular noncompaction (40, 41), atrial septal defect, coronary

Table. Classification system of congenital SOV aneurysms by Sakakibara and Konno (25)

Types of congenital SOV aneurysm	Description
I	The aneurysm originates in the left portion of the right sinus, protrudes forward and ruptures into the right ventricle near the pulmonary valve. The concurrent presence of VSD under the pulmonary valve is frequent.
II	The aneurysm originates in the mid portion of the right sinus, protrudes and ruptures into the right ventricle. A concurrent VSD is uncommon.
III	The aneurysm originates in the posterior portion of the right coronary sinus. IIIv: The aneurysm projects into the right ventricle behind the septal leaflet of the tricuspid valve after penetrating the membranous septum. IIIa: The aneurysm protrudes into the right atrium. VSD is rarely encountered.
IV	The aneurysm originates in the right portion of the noncoronary sinus and ruptures into the right atrium. A combined VSD is uncommon.

SOV, sinus of Valsava; VSD, ventricular septal defect.



Figure 12. Axial black blood cardiac magnetic resonance image demonstrates windsock like projection into the atrioventricular groove related to aneurysm from the right SOV (black arrow).

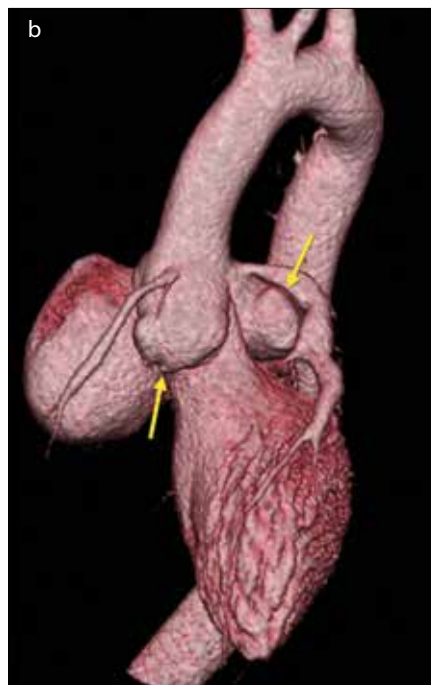
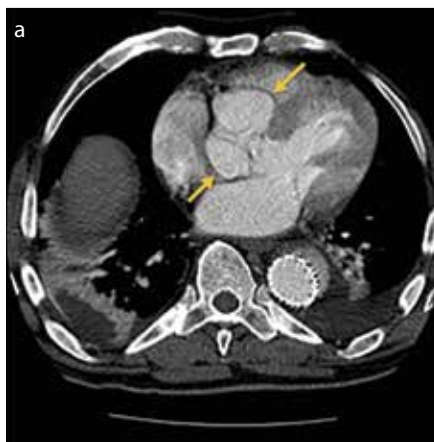


Figure 11. a, b. Saccular unruptured SOV aneurysms in a 65-year-old man. Axial CT (a) and 3D volume rendered (b) images from an ECG-gated cardiac CT angiography shows saccular aneurysms of the right and noncoronary sinuses (yellow arrows). Note is made about bilateral small pleural effusion and descending thoracic aortic graft for aneurysm repair.

anomalies (aberrant left coronary artery with separate origins of the left anterior descending and circumflex arteries) (35), left-sided superior vena cava (42), atrial septal defect (43), patent ductus arteriosus, and hypertrophic obstructive cardiomyopathy (44).

Treatment planning and management of SOV aneurysms

Surgery has been conventionally and commonly used for repair of SOV aneu-

rysms. Following successful surgical repair of a ruptured aneurysm, the prognosis is excellent with 10-year survival rates of 90%–95% (45, 46). Surgical repair is indicated for ruptured aneurysms and unruptured SOV aneurysm with associated congenital defects like VSD, or complications like aortic regurgitation, mitral valve incompetence, right ventricular outflow obstruction, infection, and myocardial ischemia (47). The three surgical routes described consist of aortotomy through the aortic root, through

ruptured cardiac chamber site of aneurysm, and combination of both (16, 48).

Recently, various percutaneous closure techniques (45, 46) are gaining popularity in certain scenarios; for example with the rupture opening site less than 9 mm in diameter and the distance between the SOV opening of the ruptured aneurysm and the coronary artery not less than 5 mm (49). Various reported closure devices used in such condition include Rashkind umbrella, septal and ductal occluder devices, and Amplatzer vascular plug (16).

Patients with unruptured, stable, or asymptomatic SOV aneurysms are usually followed clinically and with imaging. Society guidelines regarding management of aortic aneurysm in general are applicable for unruptured SOV aneurysm (48). One study of 53 cases proposed for anticoagulation of patients with unruptured stable aneurysms, and 6-monthly imaging follow-up. In this study, surgical repair was performed in the presence of symptoms, or the affected sinus size more than 50% of the average size of the other two normal sinuses, compressive or distortive effects on surrounding chambers, or with size increase on follow-up imaging (46, 50).

Conclusion

SOV aneurysm is a rare important aortic root defect, which can be a cause of some serious cardiac sequels, but easy to remain undiagnosed in busy clinical practice setting. Hence increased awareness of

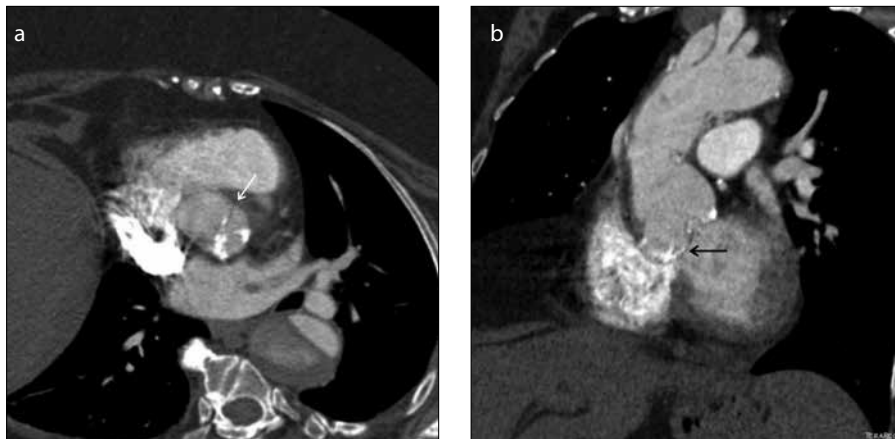


Figure 13. a, b. A 59-year-old woman with history of ascending aortic tube graft repair for Type A aortic dissection extending into descending aorta presents with SOV aneurysm. Short axis contrast-enhanced axial (a) and oblique coronal reconstructed (b) CT images through the aortic root demonstrates partially calcified bicuspid aortic valve (white arrow) and SOV aneurysm from noncoronary sinus (black arrow). Note previous type B aortic dissection in the descending aorta with partial thrombosis of the false lumen.

this entity and prompt accurate diagnosis is important, to prevent fatal event from untreated ruptured SOV aneurysm. Gated multidetector CT and MRI play an important role as noninvasive imaging modalities for their evaluation.

Acknowledgements

We thank Pam Curry, Medical Illustration Department, UT Southwestern Medical Center for her valuable help in supplying the medical illustrations and animations of this work.

Conflict of interest disclosure

The authors declared no conflicts of interest.

References

1. Takach TJ, Reul GJ, Duncan JM, et al. Sinus of Valsalva aneurysm or fistula: management and outcome. *Ann Thorac Surg* 1999; 68:1573–1577. [CrossRef]
2. Chu SH, Hung CR, How SS, et al. Ruptured aneurysms of the sinus of Valsalva in Oriental patients. *J Thorac Cardiovasc Surg* 1990; 99:288–298.
3. Hoey ET, Kanagasigam A, Sivananthan MU. Sinus of Valsalva aneurysms: assessment with cardiovascular MRI. *AJR Am J Roentgenol* 2010; 194:W495–504. [CrossRef]
4. Bricker AO, Avutu B, Mohammed TL, et al. Valsalva sinus aneurysms: findings at CT and MR imaging. *Radiographics* 2010; 30:99–110. [CrossRef]
5. Hope J. A treatise on the diseases of the heart and great vessels and on the affections which may be mistaken for them; comprising the author's view of the physiology of the heart's action and sounds, as demonstrated by his experiments on the motions and sounds in 1830, and on the sounds in 1834–5. 3rd ed., corr. and greatly enl. London: J. Churchill, 1839; 5.
6. Chang CW, Chiu SN, Wu ET, Tsai SK, Wu MH, Wang JK. Transcatheter closure of a ruptured sinus of Valsalva aneurysm. *Circ J* 2006; 70:1043–1047. [CrossRef]

7. Conde CA, Meller J, Donoso E, Dack S. Bacterial endocarditis with ruptured sinus of Valsalva and aorticocardiic fistula. *Am J Cardiol* 1975; 35:912–917. [CrossRef]
8. Goldberg N, Krasnow N. Sinus of Valsalva aneurysms. *Clin Cardiol* 1990; 13:831–836. [CrossRef]
9. Koh KK, Lee KH, Kim SS, Lee SC, Jin SH, Cho SW. Ruptured aneurysm of the sinus of Valsalva in a patient with Behcet's disease. *Int J Cardiol* 1994; 47:177–179. [CrossRef]
10. Underwood MJ, El Khoury G, Deronck D, Glineur D, Dion R. The aortic root: structure, function, and surgical reconstruction. *Heart* 2000; 83:376–380. [CrossRef]
11. Kunzelman KS, Grande KJ, David TE, Cochran RP, Verrier ED. Aortic root and valve relationships. Impact on surgical repair. *J Thorac Cardiovasc Surg* 1994; 107:162–170.
12. Troupis JM, Nasis A, Pasricha S, Patel M, Ellims AH, Seneviratne S. Sinus Valsalva aneurysm on cardiac CT angiography: assessment and detection. *J Med Imaging Radiat Oncol* 2013; 57:444–447. [CrossRef]
13. Lang RM, Badano LP, Mor-Avi V, et al. Recommendations for cardiac chamber quantification by echocardiography in adults: an update from the American Society of Echocardiography and the European Association of Cardiovascular Imaging. *Eur Heart J Cardiovasc Imaging* 2015; 16:233–270. [CrossRef]
14. Lin FY, Devereux RB, Roman MJ, et al. Assessment of the thoracic aorta by multidetector computed tomography: age- and sex-specific reference values in adults without evident cardiovascular disease. *J Cardiovasc Comput Tomogr* 2008; 2:298–308. [CrossRef]
15. McKay R, Anderson RH, Cook AC. The aorto-ventricular tunnels. *Cardiol Young* 2002; 12:563–580. [CrossRef]
16. Ott DA. Aneurysm of the sinus of Valsalva. *Semin Thorac Cardiovasc Surg Pediatr Card Surg Annu* 2006; 165–176. [CrossRef]
17. Shahrabani RM, Jairaj PS. Unruptured aneurysm of the sinus of Valsalva: a potential source of cerebrovascular embolism. *Br Heart J* 1993; 69:266–267. [CrossRef]

18. Fujiwara R, Noguchi T, Morii I, et al. Acute myocardial infarction and cardiogenic shock caused by a huge right Valsalva sinus aneurysm. *Circ J* 2014; 78:1264–1265. [CrossRef]
19. Lijoi A, Parodi E, Passerone GC, Scarano F, Caruso D, Iannetti MV. Unruptured aneurysm of the left sinus of Valsalva causing coronary insufficiency: case report and review of the literature. *Tex Heart Inst J* 2002; 29:40–44.
20. Weinreich M, Yu PJ, Trost B. Sinus of Valsalva aneurysms: review of the literature and an update on management. *Clin Cardiol* 2015; 38:185–189. [CrossRef]
21. Feldman DN, Roman MJ. Aneurysms of the sinuses of Valsalva. *Cardiology* 2006; 106:73–81. [CrossRef]
22. Hands ME, Lloyd BL, Hung J. Cross-sectional echocardiographic diagnosis of unruptured right sinus of Valsalva aneurysm dissecting into the interventricular septum. *Int J Cardiol* 1985; 9:380–383. [CrossRef]
23. White CS, Plotnick GD. Case 33: sinus of Valsalva aneurysm. *Radiology* 2001; 219:82–85. [CrossRef]
24. Yuan SM, Lavee J. Pseudoaneurysm of the native sinus of Valsalva. *Kardiol Pol* 2009; 67:291–294.
25. Alla VM, Suryanarayana PG, Thambidorai SK. Thoracic aortic pseudoaneurysm following noncardiovascular surgery: a rare complication that can mimic common chest emergencies. *South Med J* 2010; 103:1186–1188. [CrossRef]
26. Cheng TO, Yang YL, Xie MX, et al. Echocardiographic diagnosis of sinus of Valsalva aneurysm: a 17-year (1995–2012) experience of 212 surgically treated patients from one single medical center in China. *Int J Cardiol* 2014; 173:33–39. [CrossRef]
27. Hijazi ZM. Ruptured sinus of Valsalva aneurysm: management options. *Catheter Cardiovasc Interv* 2003; 58:135–136. [CrossRef]
28. Sakakibara S, Konno S. Congenital aneurysm of the sinus of Valsalva. Anatomy and classification. *Am Heart J* 1962; 63:405–424. [CrossRef]
29. Guo DW, Cheng TO, Lin ML, Gu ZQ. Aneurysm of the sinus of Valsalva: a roentgenologic study of 105 Chinese patients. *Am Heart J* 1987; 114:1169–1177. [CrossRef]
30. Pampapati P, Rao HT, Radhesh S, Anand HK, Praveen LS. Multislice CT imaging of ruptured left sinus of Valsalva aneurysm with fistulous track between left sinus and right atrium. *J Radiol Case Rep* 2011; 5:14–21. [CrossRef]
31. Moustafa S, Mookadam F, Connelly MS. Retentive uneventful rupture of right coronary sinus of Valsalva aneurysm into right ventricle. *Heart Lung Circ* 2013; 22:390–391. [CrossRef]
32. Wang KY, St John Sutton M, Ho HY, Ting CT. Congenital sinus of Valsalva aneurysm: a multiplane transesophageal echocardiographic experience. *J Am Soc Echocardiogr* 1997; 10:956–963. [CrossRef]
33. Das KM, El-Menyar AA, Arafa SE, Suwaidi JA. Intracardiac shunting of ruptured Sinus of Valsalva aneurysm in a patient presented with acute myocardial infarction: role of 64-slice MDCT. *Int J Cardiovasc Imaging* 2006; 22:797–802. [CrossRef]
34. Hoey ET, Ganeshan A, Nadar SK, Gulati GS. Evaluation of the aortic root with MRI and MDCT angiography: spectrum of disease findings. *AJR Am J Roentgenol* 2012; 199:W175–186. [CrossRef]

35. Xenikakis T, Malliotakis P, Barbetakis N, Manoussakis E, Hassoulas J. Congenital malformations of the aortic root: bicuspid aortic valve in combination with unruptured aneurysm of the left sinus of Valsalva and aberrant left coronary artery. *Hellenic J Cardiol* 2008; 49:288–291.
36. Miller SW WJ. *Problem solving in Cardiovascular imaging* Philadelphia: Elsevier, 2013; 35.
37. Abe H, Takeda N, Aoki H, Nagai R. Sinus of Valsalva aneurysm accompanying bicuspid aortic valve. *Intern Med* 2012; 51:1275. [\[CrossRef\]](#)
38. Anastasiades CP, Chee CE, Petsas AA. Infundibular ventricular septal defect, aneurysm of the sinus of Valsalva, and bicuspid aortic valve in a caucasian male. *J Am Soc Echocardiogr* 2005; 18:268–271. [\[CrossRef\]](#)
39. Pagé M MF, Stevens LM, Soulière V, Khairy P, El-Hamamsy I. aortic dilation rates in patients with bicuspid aortic valve correlations with cusp fusion phenotype. *J Heart Valve Dis* 2014; 23:8.
40. Caudron J, Dubourg B, Dacher JN. Unruptured aneurysm of the right sinus of Valsalva associated with right coronary cusp thickening and left ventricular non-compaction: insight from cardiac CT. *Diagn Interv Imaging* 2014; 95:881–883. [\[CrossRef\]](#)
41. Unlu M, Ozeke O, Kara M, Yesillik S. Ruptured sinus of Valsalva aneurysm associated with non-compaction of the ventricular myocardium. *Eur J Echocardiogr* 2008; 9:311–313.
42. Yildirim A, Batur MK, Kabakci G. Ruptured aneurysm of the sinus of Valsalva in association with persistent left superior vena cava—a case report. *Angiology* 2000; 51:167–171. [\[CrossRef\]](#)
43. Baur LH, Vliegen HW, van der Wall EE, et al. Imaging of an aneurysm of the sinus of Valsalva with transesophageal echocardiography, contrast angiography and MRI. *Int J Card Imaging* 2000; 16:35–41. [\[CrossRef\]](#)
44. Dev V, Goswami KC, Shrivastava S, Bahl VK, Saxena A. Echocardiographic diagnosis of aneurysm of the sinus of Valsalva. *Am Heart J* 1993; 126:930–936. [\[CrossRef\]](#)
45. Kerkar PG, Lanjewar CP, Mishra N, Nyayadhis P, Mammen I. Transcatheter closure of ruptured sinus of Valsalva aneurysm using the Amplatzer duct occluder: immediate results and mid-term follow-up. *Eur Heart J* 2010; 31:2881–2887. [\[CrossRef\]](#)
46. Kuriakose EM, Bhatla P, McElhinney DB. Comparison of reported outcomes with percutaneous versus surgical closure of ruptured sinus of Valsalva aneurysm. *Am J Cardiol* 2015; 115:392–398. [\[CrossRef\]](#)
47. Yan F, Huo Q, Qiao J, Murat V, Ma SF. Surgery for sinus of Valsalva aneurysm: 27-year experience with 100 patients. *Asian Cardiovasc Thorac Ann* 2008; 16:361–365. [\[CrossRef\]](#)
48. Kloppenburg GT, Sonker U, Post MC, Yilmaz A, Morshuis WJ. Emergency surgery for ruptured sinus of Valsalva aneurysms. *Scand Cardiovasc J* 2011; 45:374–378. [\[CrossRef\]](#)
49. Zhong L, Tong SF, Zhang Q, et al. Clinical efficacy and safety of transcatheter closure of ruptured sinus of Valsalva aneurysm. *Catheter Cardiovasc Interv* 2014; 84:1184–1189. [\[CrossRef\]](#)
50. Vural KM, Sener E, Tasdemir O, Bayazit K. Approach to sinus of Valsalva aneurysms: a review of 53 cases. *Eur J Cardiothorac Surg* 2001; 20:71–76. [\[CrossRef\]](#)